vaccines

MDPI

Article

Proinflammatory Innate Cytokines and Distinct Metabolomic Signatures Shape the T Cell Response in Active COVID-19

Akshay Binayke [1], Aymaan Zaheer [2,†], Jyotsna Dandotiya [1,†], Sonu Kumar Gupta [3], Shailendra Mani [3], Manas Ranjan Tripathy [2], Upasna Madan [1], Tripti Shrivastava [3], Yashwant Kumar [3], Anil Kumar Pandey [4], Deepak Kumar Rathore [3] and Amit Awasthi [1,2,*]

[1] Immunobiology Lab, Translational Health Science and Technology Institute, Faridabad 121001, India
[2] Immunology Core, Translational Health Science and Technology Institute, Faridabad 121001, India
[3] Translational Health Science and Technology Institute, Faridabad 121001, India
[4] ESIC Medical College and Hospital, Faridabad 121012, India
* Correspondence: aawasthi@thsti.res.in
† These authors contributed equally to this work.

Abstract: The underlying factors contributing to the evolution of SARS-CoV-2-specific T cell responses during COVID-19 infection remain unidentified. To address this, we characterized innate and adaptive immune responses with metabolomic profiling longitudinally at three different time points (0–3, 7–9, and 14–16 days post-COVID-19 positivity) from young, mildly symptomatic, active COVID-19 patients infected during the first wave in mid-2020. We observed that anti-RBD IgG and viral neutralization are significantly reduced against the delta variant, compared to the ancestral strain. In contrast, compared to the ancestral strain, T cell responses remain preserved against the delta and omicron variants. We determined innate immune responses during the early stage of active infection, in response to TLR 3/7/8-mediated activation in PBMCs and serum metabolomic profiling. Correlation analysis indicated PBMCs-derived proinflammatory cytokines, IL-18, IL-1β, and IL-23, and the abundance of plasma metabolites involved in arginine biosynthesis were predictive of a robust SARS-CoV-2-specific Th1 response at a later stage (two weeks after PCR positivity). These observations may contribute to designing effective vaccines and adjuvants that promote innate immune responses and metabolites to induce a long-lasting anti-SARS-CoV-2-specific T cell response.

Keywords: T cells; immuno-metabolomics; COVID-19; SARS-CoV-2; vaccine adjuvants

Citation: Binayke, A.; Zaheer, A.; Dandotiya, J.; Gupta, S.K.; Mani, S.; Tripathy, M.R.; Madan, U.; Shrivastava, T.; Kumar, Y.; Pandey, A.K.; et al. Proinflammatory Innate Cytokines and Distinct Metabolomic Signatures Shape the T Cell Response in Active COVID-19. *Vaccines* **2022**, *10*, 1762. https://doi.org/10.3390/vaccines10101762

Academic Editor: Antonella Caputo

Received: 19 September 2022
Accepted: 14 October 2022
Published: 20 October 2022

1. Introduction

T cell immune responses are indispensable in long-lasting protection against coronavirus disease-19 (COVID-19) [1–3]. Although the variants of concern (VoCs) acquired multiple mutations to evade the humoral immunity generated through vaccination, natural infection, or both, T cell immunity remained largely preserved against variants of SARS-CoV-2 [3–6]. Importantly, the memory T cell response against SARS-CoV-2 persists for a long time after antigen exposure, thus protecting from severe infection upon re-exposure to SARS-CoV-2 and its variants [7]. The frequency and magnitude of the antigen-specific T cell response could potentially affect the clinical manifestations of COVID-19 [8–10]. Therefore, it is critical to understand the factors that shape the magnitude of T cell responses during SARS-CoV-2 infections.

Antigen-presenting cells (APCs) provide secondary signals in the form of cytokines that are critical in modulating T cell activation and differentiation [11]. However, the phenotype of cytokines secreted by innate immune cells in generating a comprehensive T cell response is not clearly understood in COVID-19. Systems biology studies have shown that proinflammatory cytokines, IL-6, IL-1β, and TNF-α, originating from SARS-CoV-2 infected lungs, but not from the peripheral blood cells, contribute to COVID-19 severity [12]. Therefore, studying the systemic levels of cytokines to predict the T cell response may

prove misleading. There are limited reports of cellular innate immune responses and their correlation with adaptive immunity. A few recent longitudinal studies have documented the early innate and adaptive immune responses during mild COVID-19 [13,14]; however, no reports identify a correlation of an early innate immune response with the generation of T cell responses in active COVID-19. To address this, we used TLR 3, 7, and 8 agonists to stimulate the PBMCs isolated within three days of PCR diagnosis of mild COVID-19 patients and measured the range and magnitude of innate cytokine release, which were further correlated with the degree of virus-specific T cell responses generated during active COVID-19 in mild cases where the virus was successfully cleared. We aim to shed light on the coordination of the innate and adaptive immune responses over the course of acute COVID-19 and understand the phenotypes of the immune cells involved at each stage to gain a holistic understanding of how the different branches of the immune system act sequentially during infection.

We, and others, have reported that COVID-19 patients have altered metabolic pathways and a dysregulation of energy production [15–19]. Since plasma metabolites substantially influence the immune cells in shaping protective immune responses, we tested whether the levels of specific metabolites or metabolic pathways correlate with the antiviral immune responses. Our results reveal that the TLR-specific proinflammatory cytokine activity by PBMCs and a plasma metabolic signature correlate with a robust T cell immune response against COVID-19 infection.

2. Materials and Methods

2.1. Study Plan

To investigate the factors that contribute to the priming of a robust anti-SARS-CoV-2 T cell response, we longitudinally studied immune-metabolomic signatures during acute infection in young, mildly symptomatic COVID-19 patients infected with the SARS-CoV-2 virus in mid-2020 by collecting blood samples on day 0–3 (indicated as "V1"), day 7 (indicated as "V2"), and day 14 (indicated as "V3") from the date of PCR positive infection report. Since no COVID-19 vaccines were authorized in India at the time of sample collection for this study in mid-2020, none of the participants were vaccinated. Clinically relevant medical information (e.g., age, patient-reported symptoms) was collected at the time of enrolment. For comparison, blood was also collected from age-matched SARS-CoV-2 RT-PCR-negative healthy volunteers (Table S1). The clinical cohort was considerably young and consisted of 8 females and 13 males, with a median age of 28 years (IQR: 25:34) (Table S1). From the collected blood samples, we separated the plasma and PBMCs, which were cryopreserved until further experimentation. The humoral immune response against SARS-CoV-2 and its variants was evaluated using the plasma samples collected from the 21 patients. PBMCs from all three-time points were used to determine antigen-specific T cell response dynamics during acute COVID-19. To study the status of innate immunity against SARS-CoV-2, we ex vivo stimulated the PBMCs of V1 samples with a cocktail of TLR 3/7/8 agonists, and the released cytokines were quantified. We performed a Spearman correlation analysis of the innate immune response from V1 samples with the SARS-CoV-2-specific T cell immune response of V3. The metabolic signature obtained from the plasma was further correlated with the SARS-CoV-2-specific innate and T cell immune responses (Figure 1A).

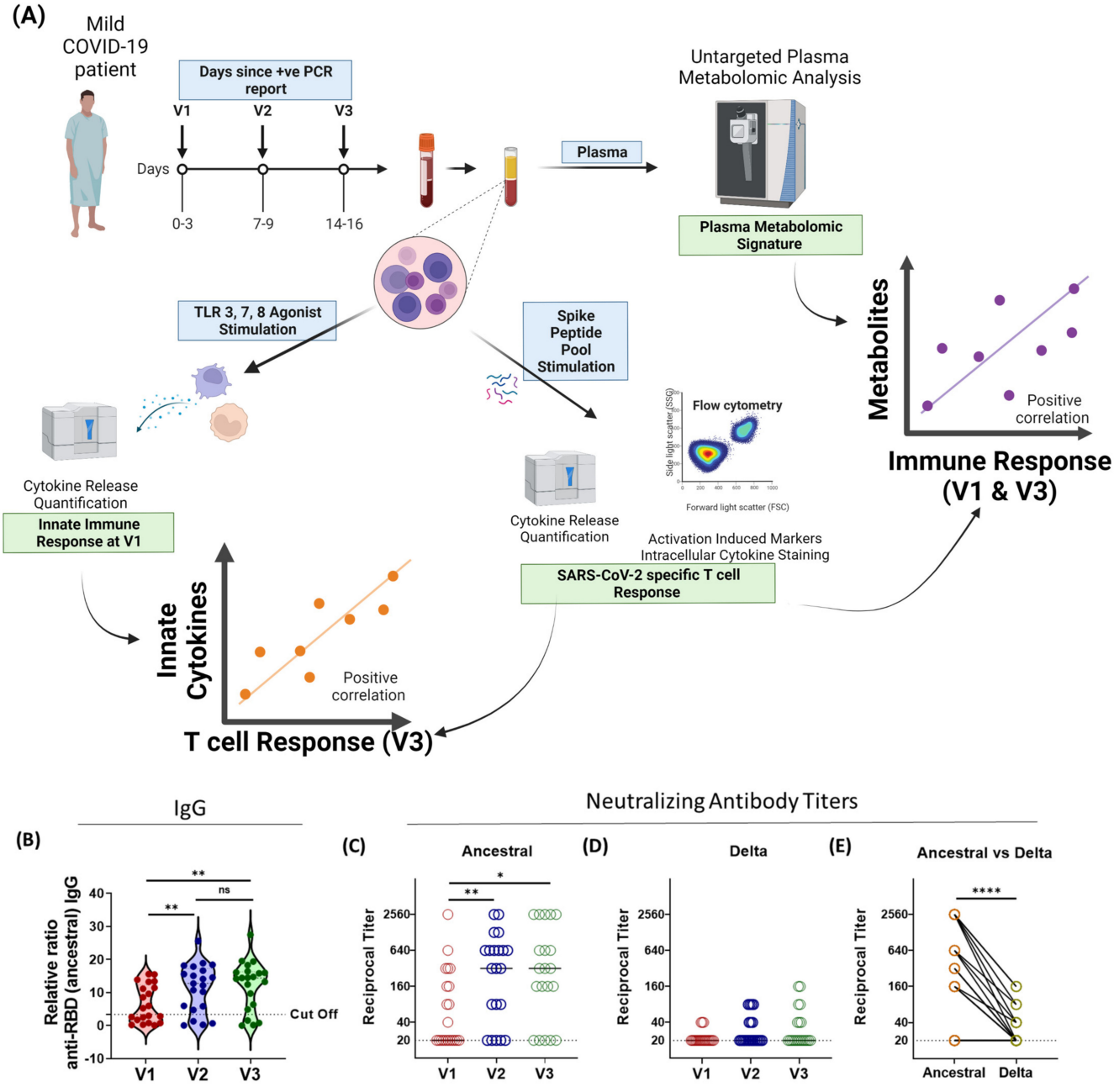

Figure 1. Longitudinal analysis of humoral immune response against the SARS-CoV-2 during acute COVID-19 infection. (**A**) Graphical representation of the study plan. (**B**) The longitudinal anti-RBD IgG responses were evaluated by performing ELISA against the RBD proteins of the ancestral (Wuhan isolate) strain. All data, represented as ratio-converted ELISA reads to a pool of pre-pandemic negative control samples (relative ratio), were plotted using violin plots. (**C**–**E**) The longitudinal neutralizing antibody titers against (**C**) the ancestral strain and (**D**) the delta strain of SARS-CoV-2 during V1 (day 0–3), V2 (day 7), and V3 (day 14) from COVID-19 positivity. (**E**) The paired representation of NAb titers in the active COVID-19 patients during V3 against the ancestral and delta variants of SARS-CoV-2. *ns* not significant * $p < 0.05$, ** $p \leq 0.01$, **** $p < 0.0001$.

2.2. Human Ethics

All the experiments were performed according to the suggested guidelines of the Institutional Ethics Committee (Human Research) of THSTI and ESIC Hospital, Faridabad (letter ref No: THS 1.8.1 (97), dated 7 July 2020). Peripheral blood samples were collected

from asymptomatic or mildly symptomatic COVID-19-positive and healthy individuals after receiving written informed consent. Individuals were enrolled in this study upon appropriate approval from the Institutional Ethics Committee (human research) of THSTI.

2.3. Peripheral Blood Mononuclear Cells (PBMC) Isolation

Venous blood from healthy participants and COVID-19 patients was collected in CPT™ tubes (BD Biosciences, Franklin Lakes, NJ, USA) and centrifuged at 1500× *g* for 25 min at 25 °C, within 2 h of blood draw. Plasma was separated from the upper layer, aliquoted, and stored at −80 °C until further use. The layer of PBMCs was transferred into a 15 mL tube and washed with sterile ice-cold PBS. The total PBMCs were counted on a hemocytometer after staining with trypan blue and were resuspended in freezing media (90% FBS + 10% DMSO), followed by storage at −80 °C for at least 24 h, before being transferred to liquid nitrogen.

2.4. THSTI In-House RBD IgG ELISA

ELISAs to detect IgG binding to receptor binding domain (RBD) were performed as previously described [20]. Positive convalescent and negative control samples were added to each plate for normalization. The assay results were normalized by dividing the blank subtracted readings of each sample by negative control to obtain the fold change reading.

2.5. Virus Neutralization Assay

Virus microneutralization assay titers were estimated as described previously [12]. Briefly, plasma samples were serially diluted from 1/20 to 1/2560 and incubated with the ancestral (Wuhan isolate) and the delta (B.1.617.2) SARS-CoV-2 isolates. The 50% neutralization values were estimated with four-parameter logistic regression.

2.6. Peptide Pool

The 15mer peptides pool with an overlap of 11 amino acids spanning the entire sequence of spike protein (157 + 158 peptides, JPT (Berlin, Germany), PepMix, Cat. No.PM-WCPV-S-1 (ancestral), PM-SARS2-SMUT06-1 (delta), and PM-SARS2-SMUT08-1 (omicron)) were used for determining the ancestral, B.1.617.2, and B.1.1.529 SARS-CoV-2 spike-specific T cell responses by AIM assay, ICS, and cytokine bead assay.

2.7. SARS-CoV-2-Specific T Cell Response

SARS-CoV-2-specific T cell responses were studied, as described previously [6,21,22]. PBMCs were stimulated with peptide pools at a 2 µg/mL/peptide concentration and with an equimolar dimethyl sulfoxide (DMSO) concentration as a negative control. Phytohemagglutinin (PHA, Roche (Mannheim, Germany); 5 µg/mL) was used as a positive control. As a co-stimulant, anti-CD28 and anti-CD49d were added (BD Biosciences, San Jose, CA, USA). The cells were cultured for 22–24 h, and monensin (GolgiStop™, BD Bioscience, San Diego, CA, USA) was added during the last six hours. After stimulation with peptides, the culture supernatant was separated and stored at <−20 °C until further use, and the cells were stained for flow cytometry. Spike-specific cytokine production was background-subtracted by the values obtained with the DMSO-containing medium, and the negative values were set to the limit of detection (LOD) (Figure S1). The stimulation index (SI) and LOD were calculated as described previously [22]; briefly, the SI was calculated by dividing the frequency of AIM+ CD4 or CD8 cells recorded in stimulated wells by the unstimulated wells.

2.8. Flow Cytometry

For flow cytometry, the stimulated PBMCs were stained for viability and surface markers (CD4 FITC, 1:100; CD8 BV510, 1:100; CD69 PE-CF594 1:100; CD137 BV-605 1:100; OX-40 PE-Cy7 1:100; all BD Biosciences) in FACS buffer (PBS supplemented with 2% FBS (Gibco, Invitrogen™, USA)) for 40 min at 4 °C. Next, cells were fixed and permeabilized using the Cytofix/Cytoperm kit (BD Biosciences, San Diego, CA, USA), according to the

manufacturer's instructions. Intracellular staining was performed by incubating the cells in perm/wash buffer supplemented with antibodies for 30 min at 4 °C (IFNγ PE, 1:50; IL-2 BV711, 1:50; TNFα BB700, 1:50; GranzymeB (GZB) PE 1:50; Perforin APC 1:100; all BD Biosciences, San Jose, CA, USA). Samples were acquired on a fluorescence-activated cell sorter (FACS) Symphony^{TM} instrument (BD Biosciences), using BD FACSuite software version 1.0.6 (BD Biosciences, San Jose, CA, USA), and analyzed with FlowJo software version VX (Tree Star, San Carlos, CA, USA). Functional profiles were deconvoluted by employing Boolean gating in FlowJo version XV (Tree Star, San Carlos, CA, USA) (Figure S1).

2.9. Metabolomic Analysis

Metabolomic profiling of plasma metabolites was performed as described previously [23–26]. The LC/MS obtained data were processed using the Progenesis QI for metabolomics (nonlinear dynamics, a Waters Company, Newcastle, UK) software using the default settings. Manual processing of the raw data by removing drugs and exposome metabolites led to the identification of 176 metabolites at all three-time points. All the statistical and functional analyses, including the PCA, heat map, pathway enrichment analysis, PLS-DA, and analysis of variance (ANOVA), were performed based on the observed peaks intensity using the online open-source software Metaboanalyst 5.0 (Montreal, QC, Canada). Before analysis, a data integrity check was performed, and the raw data were normalized by sum, log-transformed, and scaled by Pareto scaling. The volcano plots were constructed using the online available package VolcaNoseR (Amsterdam, The Netherland) [27].

2.10. In Vitro Stimulation of PBMCs with TLR Agonists

PBMCs were stimulated as previously described [12], with some modifications. Approximately one million cells were added to each well and all wells received stimulation with a viral cocktail containing 4.0 µg/mL R848 and 25 µg/mL poly I:C. Negative control DMSO stimulated cells were also cultured for each sample. The cells were incubated in a 5% CO_2 incubator at 37 °C for about 24 h, after which the culture supernatant was collected to analyze cytokine secretion.

2.11. Analysis of Cytokine Secretion by Luminex

Cytokine secretion in the cell culture supernatant was analyzed with a customized Premixed Multi-Analyte Luminex Discovery Assay kit (LXSAHM-10 (peptide pools stimulation); LXSAHM-11 (TLR agonist stimulation); R&D systems, Minneapolis, MN, USA). The assays were performed as per the manufacturer's instructions. The analytes examined upon peptide pool stimulation were Granzyme B, IL-2, IL-5, IL-12 p70, IL-23, IFN-gamma, IL-4, IL-6, IL-17/IL-17A, and TNF-alpha, whereas the analytes examined upon TLR stimulation were IL-23, IFN-gamma, IL-6, IL-12 p70, TNF-alpha, IL-33, IL-8, IL-10, CCL2, IL1-beta, and IL-18.

2.12. Data Representation and Statistical Analysis

The statistical analysis and data representation were performed using GraphPad Prism 9.0 (San Diego, CA, USA) and FlowJo XV (Tree Star, San Carlos, CA, USA) unless otherwise stated. The antibody responses were compared using the RM one-way ANOVA Tukey's multiple comparison test. The cytokine and T cell responses against each variant versus ancestral strain and at different stages of acute infection were calculated and compared using the Wilcoxon matched-pairs signed-rank test. T cell responses were calculated as background-subtracted data by subtracting the values obtained from the SARS-CoV-2 peptide pool stimulation from the DMSO stimulation. Negative values were set to the LOD. The cytokine secretion response upon peptide or TLR stimulation was calculated as fold change data for the correlation analysis by dividing the stimulated wells by unstimulated wells of the same sample. The correlation between the innate and adaptive immune response was performed using the Spearman correlation test. For metabolomic analysis, processing the raw data by removing drugs and exposome metabolites led to the identification of

176 metabolites at all three stages (visit 1, visit 3, and healthy control). All the statistical and functional analyses, including the PCA, heat map, pathway enrichment analysis, PLS-DA, and analysis of variance (ANOVA), were performed based on the observed peaks intensity using the online open-source software Metaboanalyst 5.0 (Montreal, QC, Canada). Before analysis, a data integrity check was performed, and the raw data were normalized by sum, log-transformed, and scaled by Pareto scaling (Figure S4). The volcano plots were constructed using the online available package VolcaNoseR (Amsterdam, Netherland) [27].

A broadscale Spearman correlation analysis of the metabolites belonging to the V1 and V3 groups with the innate and adaptive immune responses of V1 and V3 was performed. Those metabolites belonging to V1 and V3 that significantly correlated ($p < 0.05$, $r > 0.45$) with the proinflammatory innate immune responses and/or TH1 skewed T cell immune responses, and pathway library of KEGG were selected for pathway analysis using the Metaboanalyst 5.0 software (Montreal, QC, Canada) [28]. The graphical abstract and Figure 1 were prepared using Biorender.com (accessed on 19 September and 20 October 2022).

3. Results

3.1. Humoral Immune Responses against SARS-CoV-2 Variants Is Broadly Inadequate in Active-COVID-19 Patients

To study the kinetics of the antibody response against SARS-CoV-2, we first investigated the IgG response against the SARS-CoV-2 RBD protein using enzyme-linked immunosorbent assays (ELISAs). For all assays, blank-subtracted colorimetric values were normalized to a pre-pandemic negative control plasma sample, added to each assay plate, and expressed as ratios to this pool of negative samples, as described previously [29]. We observed that the anti-RBD (ancestral) IgG titers increased about three-fold by V2 and V3, compared to V1 (Figure 1B). However, similar to the previous reports in vaccinated and convalescent individuals [30], the cross-reactive antibody response against the RBD proteins of the delta (B.1.617.2), beta (B.1.315), and alpha (B.1.1.7) variants was significantly reduced (Figure S3). While the median neutralizing antibody (NAb) titers increased significantly by V2 and V3, as compared to V1, against the ancestral virus (Figure 1C), cross-reactive NAb titers against the delta variants were found to be significantly decreased at V2 and V3, as compared to the ancestral virus ($p < 0.0001$, Figure 1E). We observed that, even by V3, only 33% (7/21) individuals had detectable levels of cross-reactive NAbs against the delta variant (Figure 1D). Therefore, in concurrence with the previous reports, the cross-reactive antibody-mediated protection against different variants of SARS-CoV-2 in active COVID-19 patients infected with ancestral strain is broadly inadequate.

3.2. Spike-Specific T Cell Response in COVID-19 Patients

We studied the antigen-specific T cell response from the PBMCs of active COVID-19 patients by stimulating them with peptide pools spanning the entire length of the spike protein for 20–24 h. The T cell response upon peptide pool stimulation was measured by calculating the expression of T cell receptor (TCR)-dependent activation-induced markers (AIM) [10] and Th1 cytokines after background subtraction from DMSO stimulated wells [31]. The CD4+ T cells co-expressing CD137 and OX-40 are designated as CD4+ AIM+ cells (Figure 2A), and the CD8+ T cells co-expressing CD137 and CD69 are defined as CD8+ AIM+ cells (Figure 2B) [10,21].

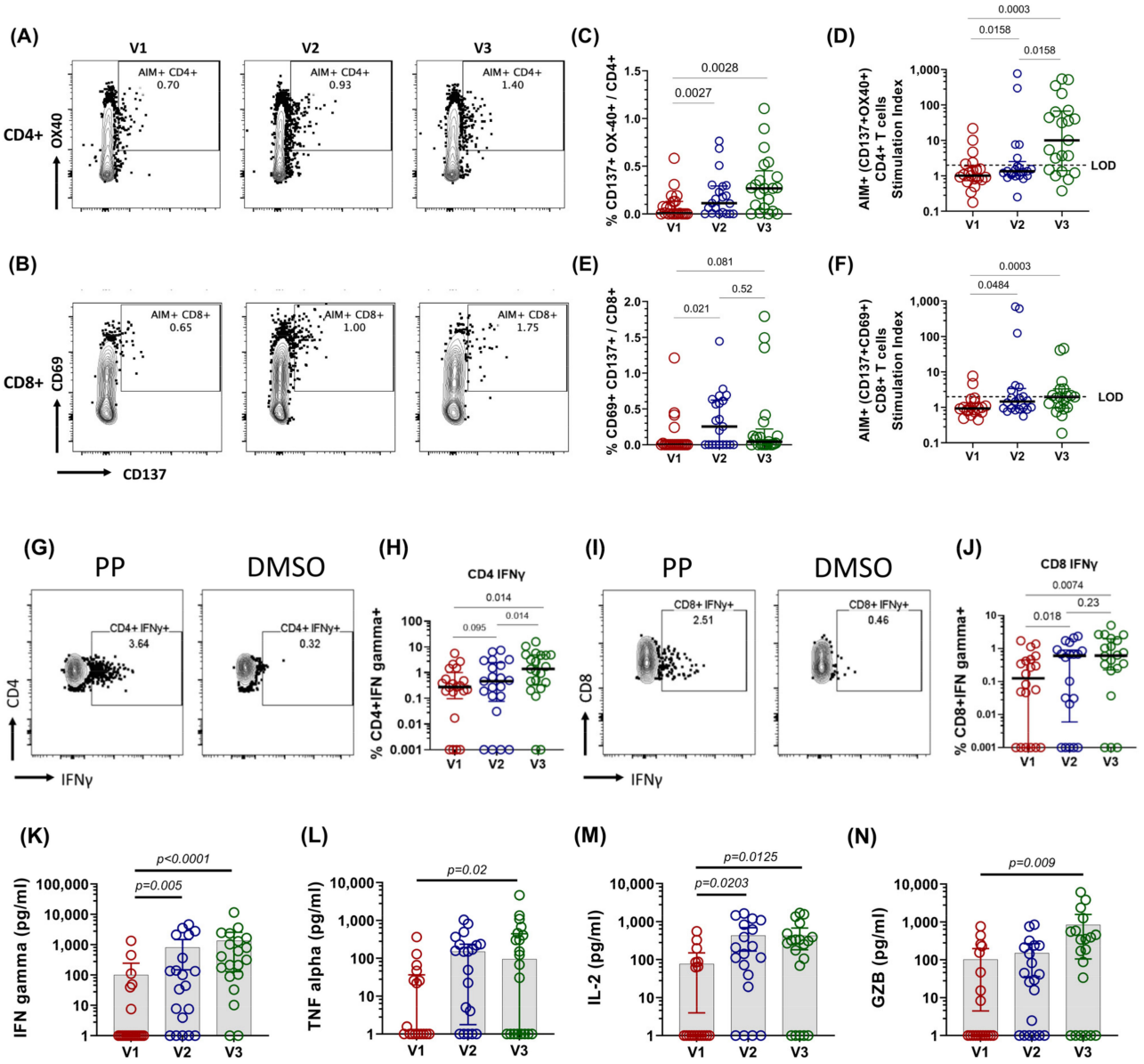

Figure 2. Longitudinal dynamics of antigen-specific T cell immune responses during COVID-19 infection. Representative flow cytometry plots of SARS-CoV-2 spike-specific T cells expressing activation-induced markers (AIM) (**A**) CD4+ (CD137 + OX40+), (**B**) CD8+ (CD137 + CD69+). (**C**–**F**) Longitudinal analysis of the AIM response in paired samples from the same subject. (**C**) Percentage frequency of CD4+ AIM+ cells. (**D**) Stimulation index (SI) of CD4+ AIM+ cells. (**E**) %frequency of CD8+ AIM+ cells (**F**) SI of CD8+ AIM+ cells. (**G**,**I**) Representative flow cytometry plots for the intracellular cytokine staining (ICS) assay of cells upon stimulation with spike peptide pool, compared to the DMSO. Longitudinal analysis of the frequency (percentage of total CD4+ or CD8+ cells) of IFN-γ+ cells in paired samples from the same subject. (**H**) CD4+ interferon gamma (IFNγ). (**J**) CD8+ interferon gamma. Each datapoint shown is background-subtracted (DMSO stimulated wells), and line represents median values for each time point. Two-sided Wilcoxon signed rank tests were employed for paired non-parametric analysis. LOD = limit of detection for AIM assay was SI < 2. (**K**–**N**) Longitudinal dynamics of antigen-specific cytokine release by PBMCs during COVID-19 infection. (**K**) IFNγ; (**L**) TNFα; (**M**) IL-2; (**N**) granzyme B. Graphs represent longitudinal cytokine released (background-subtracted) by paired PBMC samples from the same subject upon stimulation with SARS-CoV-2 spike peptide pool for 22–24 h. Bars represent median values with IQR.

The expression of activation-induced markers (AIM) in the CD4+ T cells were observed as early as V1 (6/21), which may be attributed to pre-existing cross-reactive T cells from prior common cold coronavirus infections [32]. The magnitude of SARS-CoV-2-specific CD4+ T cells increased significantly by V2 (day 7, $p = 0.0027$) and by V3 (day 14, $p = 0.0028$) (Figure 2C). Consistent with previous reports [10], the AIM+ cells in CD4+ T cells were observed in ~76% of the patients by V3 (16/21) (Figure 2D). Likewise, AIM+ spike-specific CD8+ T cells were detected as early as V1 (4/21). Interestingly, unlike CD4+ T cells, the frequency and magnitude of AIM+ cells in CD8+ T cells peaked quickly from V1 to V2 ($p = 0.021$) and did not change significantly from V2 to V3 ($p = 0.52$) (Figure 2E). Antigen-specific CD8+ T cells were detected in only 57% (12/21) (Figure 2F) of the patients at V3, in line with the previous findings reported by Moderbacher et al., 2020 [10].

The functional antigen-specific T cell response was tested by the intracellular expression of IFN-γ and IL-2 by performing intracellular cytokine staining of spike peptide pool-stimulated PBMCs. Similar to the CD4+ AIM+ response, the CD4+ IFN-γ+ cell frequencies increased significantly from V1 to V3 ($p = 0.014$, Figure 2G,H). Likewise, the functional SARS-CoV-2-specific cytotoxic T cell frequency, characterized by CD8+ IFN-γ+ cell frequency, increased significantly from V1 to V3 ($p = 0.0074$, Figure 2I,J). Therefore, to summarize, we found a steady increase in the CD4 and CD8 AIM and functional T cell response, which was identified by the intracytoplasmic expression of IFN-γ in both CD4+ and CD8+ T cells.

To further understand the range of cytokines released after the stimulation of PBMCs with the peptide pool, the release of cytokines was calculated by cytokine bead assay (Figure S6). With the progression of time, we observed a steady increase in the secretion of Th1-specific cytokines, such as IFN-γ (mean: V1:100 pg/mL; V2: 810 pg/mL; V3: 1352 pg/mL, Figure 2K), TNFα (mean: V1: 40 pg/mL; V2: 206 pg/mL; V3: 478 pg/mL, Figure 2L), and IL-2 (mean: V1: 77 pg/mL; V2: 430 pg/mL; V3: 429 pg/mL, Figure 2M), whereas Th-2- and Th-17-specific cytokines did not change significantly (Figure S7A,C,D). We did not detect any notable differences in the IL12p70 secretion (Figure S7E), but as the antigen-specific T cell response increased, the proinflammatory cytokines IL-23 and IL-6 upon antigen exposure increased significantly by visit 3 (IL-6: mean:898 pg/mL; $p = 0.013$; IL-23: mean: 711 pg/mL; $p = 0.034$, Figure S7B,F). The cytotoxic response, evaluated by the levels of granzyme B, also increased extensively at V3, compared to V1 ($p = 0.009$, mean V3 = 841 pg/mL, Figure 2N).

To summarize, the SARS-CoV-2-specific T cell immune responses were predominated by Th1 cytokine expression, and their magnitude progressively increased with the advent of time after antigen exposure.

3.3. Cross-Reactive Spike-Specific T Cell Response against Delta and Omicron Variants Is Largely Preserved in Active COVID-19 Patients

We found that the antigen-specific T cell response is significantly increased by 14 days post-detection of COVID-19 infection with the ancestral strain. To confirm whether the T cell responses elicited by the ancestral strain in active COVID-19 patients could cross-react with the delta and omicron spike proteins, we tested and compared the T cell response in the PBMCs (n = 24) of active COVID-19 patients exposed to the ancestral strain of SARS-CoV-2, from V2 and V3, against the spike peptide pools of the ancestral, delta, and omicron variants (Figure 3). We observed that the cross-reactive T cell response is largely preserved, with a slight reduction against the delta (1.3-fold) and the omicron (1.5-fold) spike proteins, compared to the ancestral spike. Compared to the ancestral response, the geometric mean of the AIM+ CD4+ response was reduced by 31% against delta ($p = 0.0162$) and 58% against omicron spike ($p = 0.0005$) (Figure 3A). However, the functional profile remained broadly comparable among the variants, as determined by the expression of intracellular cytokines IFN-γ, IL-2, and TNFα (Figure 3B–D).

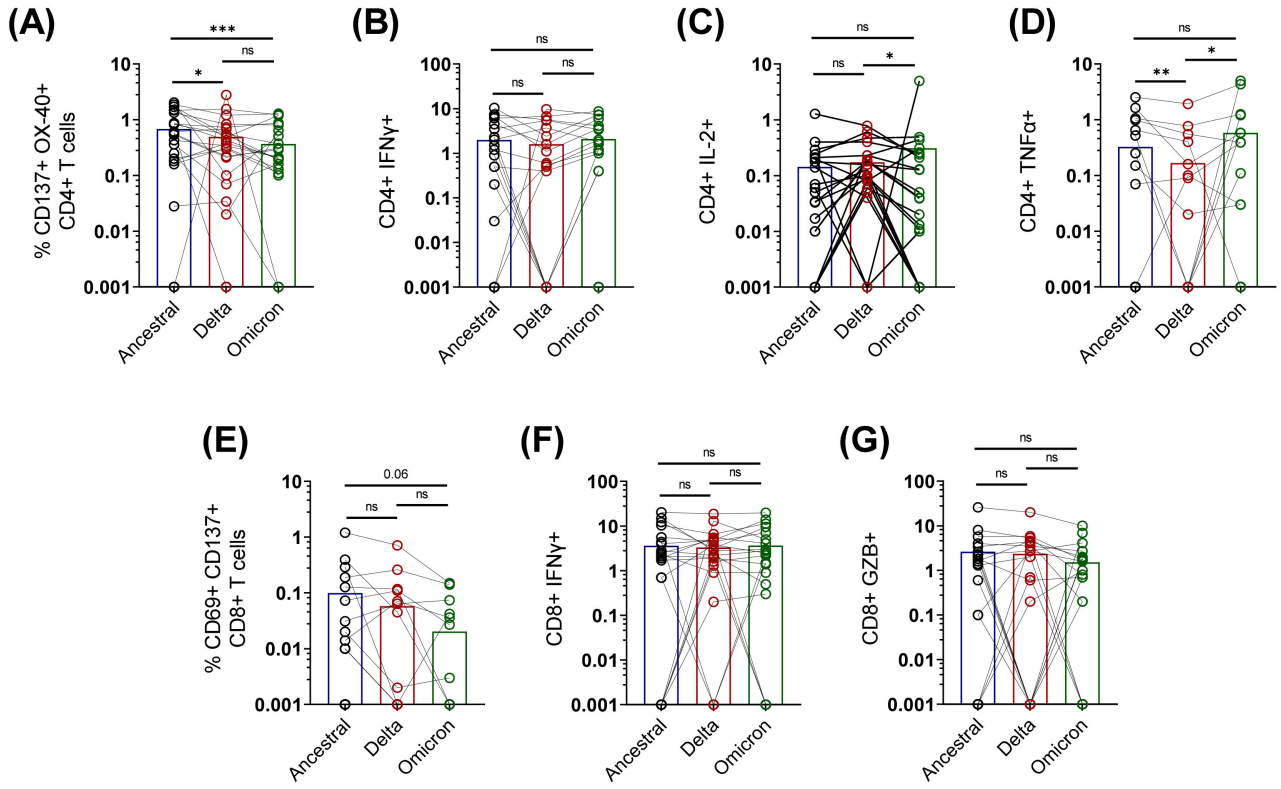

Figure 3. Cross-reactive CD4+ and CD8+ T cell response against delta and omicron spike in acute COVID-19 patients; spike-specific T cell responses in selected samples of active COVID-19 patients (n = 24) were simultaneously tested for reactivity against spike peptide pools of ancestral, delta, (B.1.617.2), and omicron (B.1.1.529). (**A**–**D**) Frequencies of antigen-specific CD4+ T cell responses: (**A**) CD4+ AIM (CD137 + OX40+); (**B**) CD4+ IFNγ; (**C**) CD4+ IL2; (**D**) CD4+ TNFα. (**E**–**G**) Frequencies of antigen-specific CD8+ T cell responses: (**E**) CD8+ AIM (CD137 + CD69+); (**F**) CD8+ IFNγ; (**G**) CD8+ granzyme B. Bars represent median values with IQR, each dot represents an individual sample, and the solid line connects the same sample stimulated with different peptide pools. Two-sided Wilcoxon signed rank tests were employed for paired non-parametric analysis. AIM, activation-induced markers; GZB, granzyme B; *ns* not significant * $p < 0.05$, ** $p \leq 0.01$, *** $p < 0.001$.

Although the geometric mean of the antigen-specific CD8+ AIM response was reduced by three- and five-fold in the delta and omicron variants, respectively, the difference was non-significant (Figure 3E). Moreover, the functional phenotypes of the antigen-specific CD8 T cells were comparable among the VoCs, compared to the ancestral spike antigen (Figure 3F,G).

Taken together, in concordance with the previous reports [3–6], the cross-reactive T cell immune responses persisted, despite the humoral immune response being abrogated against the VoCs in actively infected individuals. Our results imply the importance of the cellular immune responses against COVID-19. Thus, it is essential to further understand what factors determine the generation of a robust T cell response during active COVID-19.

3.4. Early Proinflammatory Innate Cytokine Response Correlates with a Robust T Cell Response

Next, we tested which innate immune responses correlate with adaptive immunity, especially the T cell immune response in active COVID-19 patients. Given earlier findings that COVID-19 infection impairs the APCs, such as the pDCs and myeloid cells [12,33], we wanted to test what functional phenotype of APCs correlates with the virus-specific T cell responses. We performed ex vivo stimulations of V1 PBMCs of our COVID-19 cohort, with a cocktail of synthetic agonists of toll-like receptors (TLRs) 3, 7, and 8, which are known to sense virus-derived molecules and initiate an antiviral response [34]. In the presence and

absence of the TLR agonists cocktail of poly I:C (TLR3) and R848 (TLR 7/8), the PBMCs were cultured for 24 h, as described previously [12]. The release of cytokines, such as IL-18, IL-23, IL-1β, IL-6, IL-33, IL-8, IL-10, CCL2, IL12p70, and IFNγ, in the culture supernatant was estimated by a magnetic bead-based cytokine assay. The cytokine levels in the TLR-stimulated wells were significantly higher than in the unstimulated wells (Figure S2). Therefore, to account for the differences in the number of PBMCs cultured, the fold change in the cytokine response was evaluated by dividing the cytokine response in the stimulated wells by unstimulated wells. The fold change in cytokine expression of TLR stimulated samples, compared to the unstimulated wells, was correlated with the antigen-specific T cell responses, such as the AIM markers, ICC-cytokines, and the cytokines expressed in the culture supernatant (such as TNFα, IFNγ, IL-6, IL-4, IL-17, IL-2, IL-5, IL-12p70, GZB, and IL-23 by PBMC samples from V3 upon peptide pool stimulation) (Figure 4A).

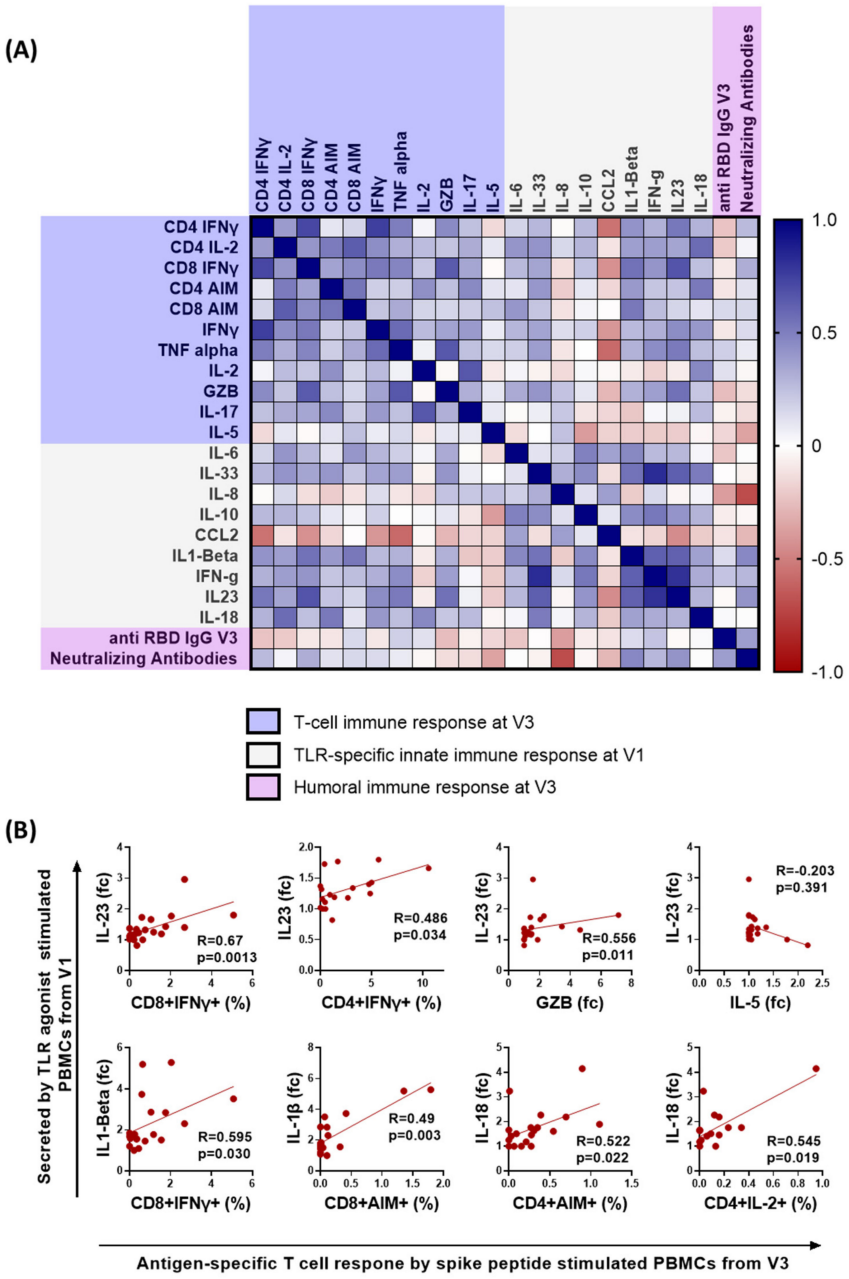

Figure 4. Correlation of early innate and adaptive immune responses in active COVID-19 patients.

Correlation between the cytokine released upon TLR agonist stimulation of PBMCs from early stages of COVID-19 infection (V1) and the magnitude of adaptive immune responses during the later stages of COVID-19 disease (V3). (**A**) A heatmap of Spearman correlation analysis; the blue rectangle depicts the analysis of stimulated PBMCs using flow cytometry or the fold change of cytokines released in the culture supernatant upon peptide stimulation; the grey rectangles represent the fold change of the cytokines released in the culture supernatant upon stimulation with TLR agonists, poly I:C (25 μg/mL) and R848 (4 μg/mL) for 24 h, and the lavender rectangle represents the humoral immune response at V3. (**B**) XY correlation plots, where the y axis represents the fold change of cytokines secreted upon TLR agonist stimulation of PBMCs from V1, and the x-axis represents the antigen-specific T cell response evaluated upon peptide pool stimulation of PBMCs from V3. Spearman correlation coefficient (R) is indicated. fc, fold change—obtained by dividing the cytokine concentration in stimulated wells by unstimulated wells; GZB, granzyme B.

The intracellular cytokine levels were highly correlated with the cytokines in the culture supernatant, indicating the robustness of the sample analysis (Figure 4A). For example, the CD4+ and CD8+ T cell IFN-γ significantly correlated with the IFN-γ levels in the culture supernatant (CD4: r = 0.751, p = 0.00014; CD8: r = 0.522, p = 0.0181; Figure 4A). The Spearman correlation analysis showed that the PBMCs from individuals that secreted a heightened proinflammatory cytokine response, in the form of IL-18, IL-1β, and IL-23, upon TLR stimulation during the early time-point of infection (V1) correlated significantly with the spike-specific T cell immune response, in the form of the expression of CD4 and CD8 IFN-γ, CD4 and CD8 AIM, and Granzyme B (GZB) secretion (Figure 4B). In contrast, the remaining cytokines, such as IL-8, CCL2, and IL-10, did not correlate. Moreover, the proinflammatory cytokines did not associate with non-Th1 cytokines, such as the IL-5, IL-17, and humoral immune responses (Figure 4A,B). Although we observed a significant negative correlation between the neutralizing antibody response and the fold change in IL-8 secretion upon TLR stimulation (r = −0.7, p = 0.0012), the observations were not further evaluated because IL-8 expression was not significantly altered upon TLR cocktail stimulation (Figure S2). To sum up, individuals exhibiting a proinflammatory functional phenotype of innate immune cells during the early stages of infection tend to develop robust antiviral T cell immunity.

3.5. Distinct Metabolomic Alterations Characterize Acute COVID-19 Infection

The correlation between metabolic profiles with innate and adaptive T cell responses in active COVID-19 infection remains unexplored. Moreover, altered metabolites in active COVID-19 patients might help predict the disease outcome and anti-SARS-CoV-2 immune responses. To determine the metabolic landscape in active COVID-19 patients, we performed a plasma metabolomic analysis to identify changes throughout COVID-19 infection. Multiple reports have identified metabolomic alterations during COVID-19 [35–38]. To obtain a broad view of the metabolic status, we studied the longitudinal plasma metabolite profile in our cohort of 21 COVID-19 patients and compared them with the plasma of 12 healthy volunteers (Table S1). The plasma samples from V1 and V3 were processed for UHPLC–MS/MS analysis, and 240 different metabolites were identified. These 240 metabolites were further screened to remove drugs and other artificial compounds and derivatives to obtain 176 metabolites. Unsupervised PCA analysis of the metabolites in our patient cohort displayed a clear distinction that separated the control (healthy individuals), COVID-19 early time point (V1), and late time point (V3) individuals (Figure 5A). The partial least squares–discriminant analysis (PLS-DA) was employed to identify the top 15 important metabolites across the three different groups (Figure 5B). Moreover, hierarchical clustering of the top 50 metabolites showed a notable shift in the metabolic signature among acute COVID-19 patients, compared to the healthy individuals (Figure 5C). The PLS-DA and hierarchical clustering analyses pointed out that the metabolites and derivatives of the citric acid cycle, such as citrate, itaconate, and trans-aconitate, were significantly reduced in COVID-19 patients (Figure 5B,C). In contrast, metabolites, such as glutamic acid

derivatives pyroglutamate and N-methyl-L-glutamic acid, were enriched in the plasma of COVID-19 patients (Figure 5B,C). Of the 176 metabolites, 158 were significantly differentiated in COVID-19 patients (FDR < 0.001), exhibiting a distinct metabolic profile. Pathway enrichment analysis using the KEGG database showed that the metabolites involved in the phenylalanine metabolism, arginine and proline metabolism, etc., were significantly altered during COVID-19 (Figure 5D). While comparing the metabolic profile during the early and later stages of infection, 33 metabolites were significantly down, and 13 were significantly up (p = 0.001, FC > 1.5, Figure 5E).

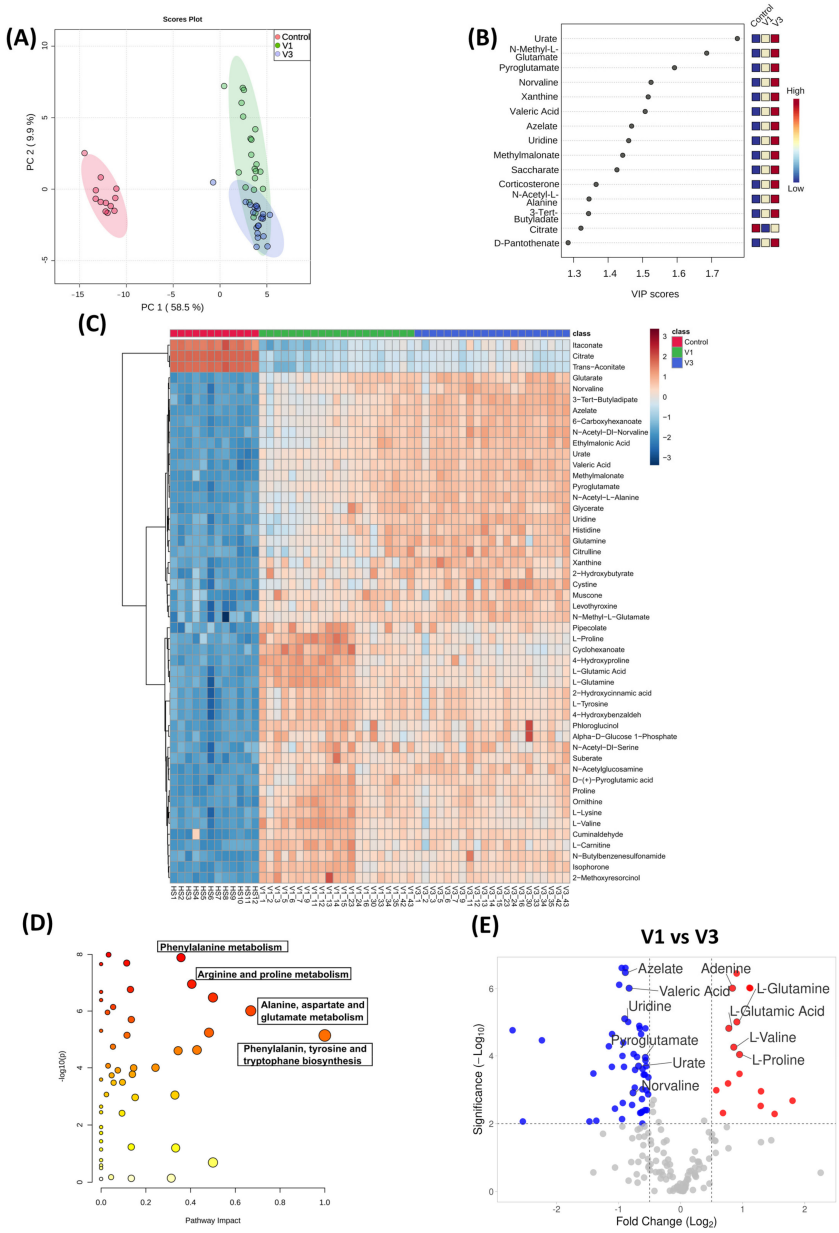

Figure 5. Metabolomic analysis of SARS-CoV-2 patient plasma samples, compared to age-matched healthy controls. (**A**) Principal component analysis of the untargeted metabolites of the three groups. (**B**) Important features identified by PLS-DA. The colored boxes indicate relative concentrations of designated metabolites in each study group. (**C**) Hierarchical cluster analysis is shown as a heatmap of the top 50 metabolites (FDR < 0.05). (**D**) Pathway enrichment analysis using KEGG of all the metabolites (n = 158) significantly altered during COVID-19 infection. (**E**) Volcano plot comparing the significantly changed (p = 0.001, FC > 1.5) metabolites during the early (V1) and later stages of disease (V3).

To understand the immune-metabolomic interaction, we performed a Spearman correlation of metabolites with innate and adaptive immune responses in COVID-19 patients and shortlisted the significantly correlating metabolites ($r > 0.45$, $p < 0.05$). Pathway analysis of the plasma metabolites that significantly correlated with the virus-specific innate immune response from V1 showed enrichment of the metabolites involved in arginine biosynthesis, D-glutamine, and D-glutamate metabolism, glutathione metabolism, histidine metabolism, etc. (Figure 6A). Similarly, pathway analysis of the metabolites that significantly correlated with the antigen-specific T cell responses at V3 displayed enrichment of the metabolites involved in arginine biosynthesis, arginine and proline metabolism, purine metabolism, etc. (Figure 6B). Notably, the normalized levels at V1 and V3 of metabolites involved in arginine and proline biosynthesis and metabolism, such as L-arginine, L-proline, L-ornithine, L-citrulline, α-ketoglutarate, L-glutamine, and L-glutamate, were significantly correlated with the innate and T cell immune responses (Figure 6C).

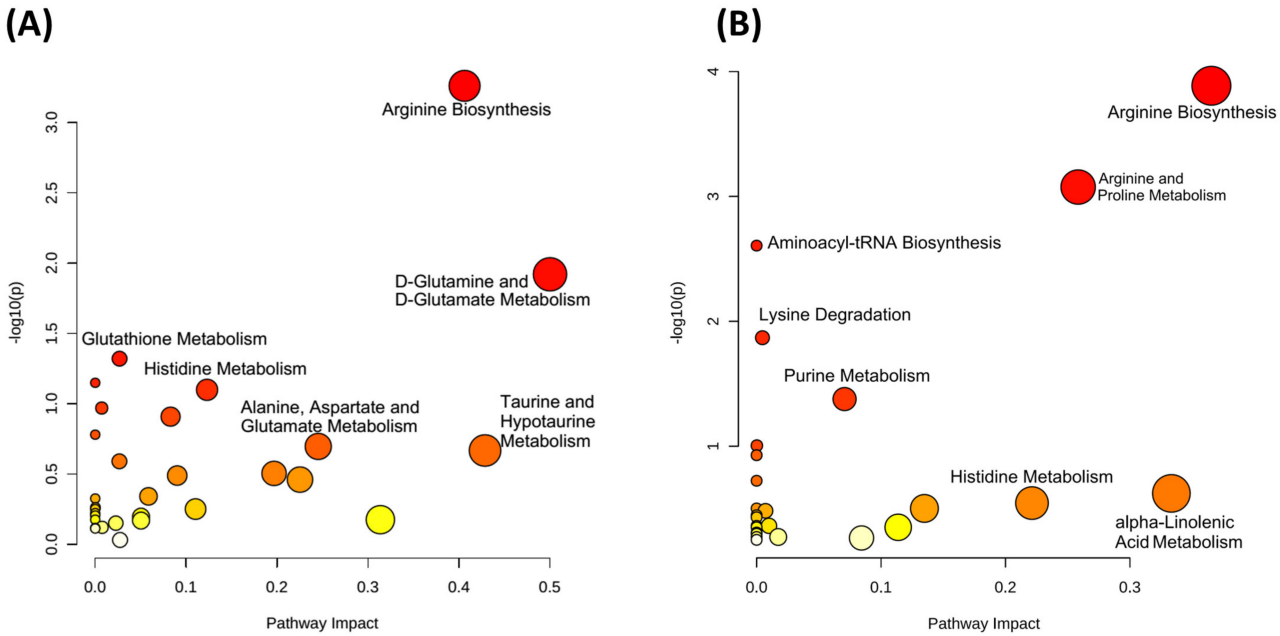

Figure 6. *Cont.*

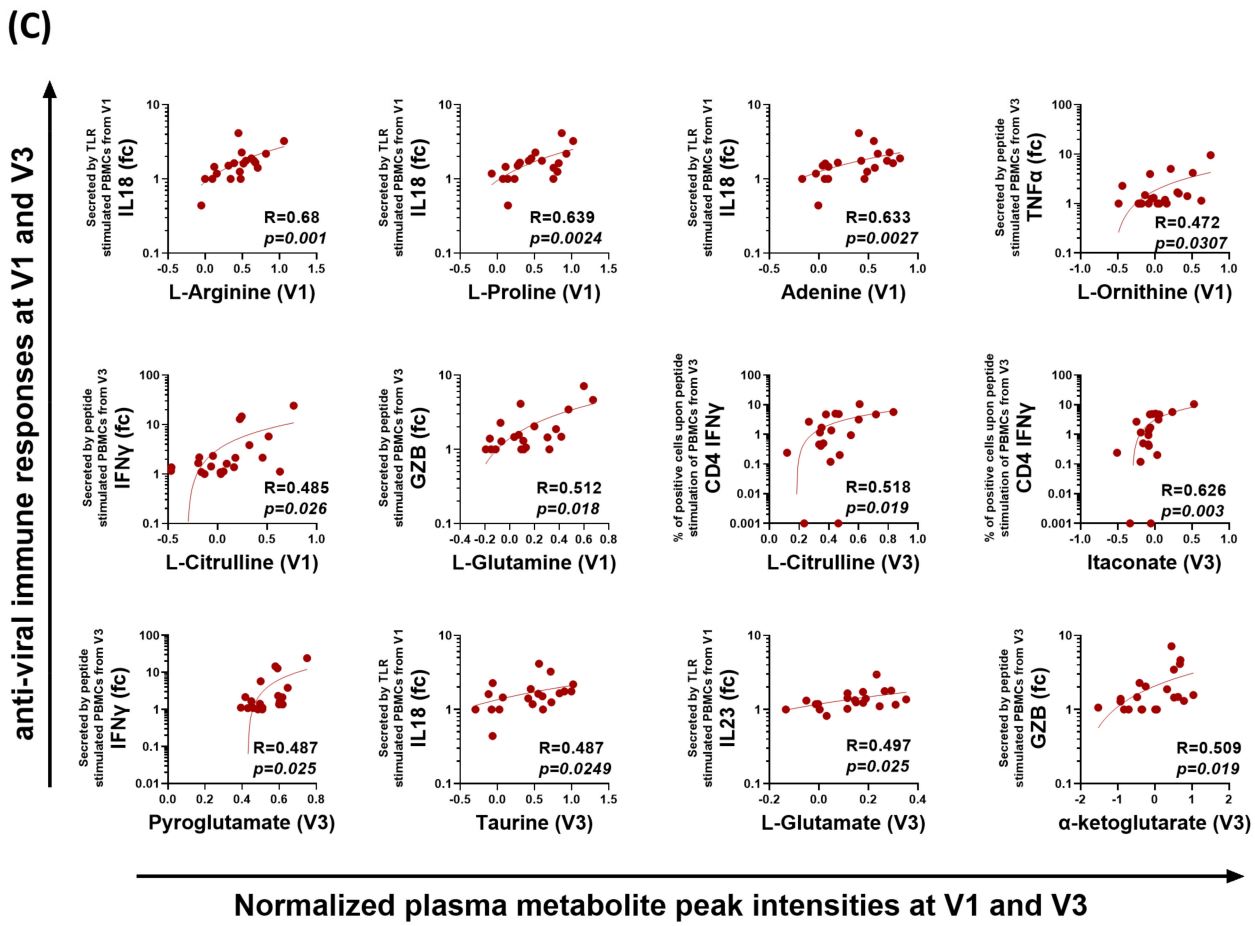

Figure 6. Correlation of metabolites with immune responses. Pathway analysis of plasma metabolites that significantly correlated ($r > 0.45$, $p < 0.05$) with (**A**) the TLR cocktail-induced innate immune response (V1) and (**B**) the T cell immune response (V3). (**C**) Representative correlation plots of metabolites from V1 and V3 that correlate with the cytokine release responses from TLR stimulated innate- and peptide pool-stimulated T cell immune responses. Each dot represents an individual sample. Spearman correlation coefficient (R) is indicated. GZB, granzyme B; fc, fold change–obtained by dividing the cytokine concentration in stimulated wells by unstimulated wells.

4. Discussion

No other viral disease in the history of humanity has been studied and reported to the extent of COVID-19. Nor has any disease in recent history caused the socio-economic devastation of life on such a global scale [39]. Several integrative studies have attempted to understand the immune correlates of protection against COVID-19 [40–42]. These studies have shown that the late induction of T cell responses [43], impaired type I interferon response [44,45], and weakened innate immune responses are immune hallmarks of severe COVID-19 [12,40].

In this study, the samples were collected during the first wave of COVID-19 (between 7 July and 4 September 2020), before the existence of delta and omicron VoCs or any COVID-19 vaccine, which allowed us to determine how T cells primed with the ancestral strain react with the spike antigen of delta and omicron variants. Although the cross-reactive antibody response is severely hampered against the variants of SARS-CoV-2, the T cell response remains largely preserved against delta [21,46], omicron [4–6,47,48], and its sub-lineages [49]. Our analysis suggests that, despite ten mutations in the delta spike [50] and more than 30 mutations in the omicron spike [51], 96% each of dominant CD4 and CD8 epitopes are conserved against the delta spike protein, whereas 80% and 82% of the CD4 and CD8 dominant epitopes, respectively, are conserved against the omicron spike

(Table S2). Therefore, the majority of the dominant T cell epitopes remain conserved. Thus, the T cells primed with the conserved epitopes of the ancestral strain will cross-react with the preserved epitopes of the emerging variants of SARS-CoV-2. The magnitude of the antigen-specific T cell response against the ancestral spike in our study was similar to previous reports [7,10]. Furthermore, we observed that the T cell response elicited during the active ancestral SARS-CoV-2 infection persists, but is relatively reduced against the delta and omicron variants, compared to the ancestral spike. The extent of reduction in the magnitude of the T cell response against VoCs is more prominent in our cohort than in previous reports in vaccinated individuals [4,5,47]. This observation could be because the overall magnitude of T cell response is low in acute samples [7] and, therefore, may have resulted in a limited scope for cross-reactivity against the VoCs.

The antigen-specific T cell response in actively infected COVID-19 patients was predominated by a Th1 phenotype with a significant increase in cytokines, such as IFN-γ, TNF-α, and IL-2 by V3. In contrast, no difference was observed in the secretion of the Th2 cytokines IL-5 and IL-4. In line with this, previous studies [7,10] have indicated minimal Th2 response in active COVID-19 and vaccinated individuals, further supporting our observations. The Th1/Th2 balance plays an essential role in the evolution of disease pathogenesis. Our observation of a Th1 skewed antigen-specific T cell response aligns with previous reports in mildly symptomatic COVID-19 patients [52].

Given the importance of T cell responses in limiting disease severity and protecting against emerging variants, the next generation of vaccines must primarily focus on the magnitude of T cell responses generated upon vaccination. However, limited studies have investigated the factors contributing to robust T cell immune responses during COVID-19. When this study was designed, minimal information was available about the innate and adaptive immune response against the SARS-CoV-2 infection. Moreover, reports indicated that severe COVID-19 patients show dysregulated innate and T cell responses [53]. Furthermore, the T cell response was delayed and sub-optimal in severe COVID-19 patients [10]. Since the study's primary objective was to elucidate the factors contributing to the generation of a robust T cell response, our cohort comprised asymptomatic or mildly symptomatic COVID-19 patients. Further studies may be performed to compare these factors between mild and severe COVID-19 patients.

For the differentiation and activation of functional T cells, the antigen-presenting cells (APCs) must provide three signals to the T cells. One is via direct TCR–MHC interaction, the second is through cognate interaction of adhesion molecules, and the third is by cytokine signaling [11]. Therefore, cytokines play a critical role in shaping the T cell response during exposure to a foreign antigen. Type I interferons are the first line of innate defense against viral pathogens. Induction of a type I interferon response early on in infection has been shown to be associated with survival in COVID-19 cases [54]. In line with this, individuals with high titers of autoantibodies against type I IFN were highly susceptible to COVID-19 mortality [55]. Furthermore, another combinatorial study reported a temporary increase of IFN-β and IP10/CXCL10 levels, associated with a dominant SARS-CoV-2-specific CD4 T cell response [13]. In contrast, administering type I interferon to COVID-19 patients at a late time point did not affect their recovery [56]. An integrative study reports that the type I interferon response does not correlate with the anti-viral T cell responses [14]. Therefore, considerable evidence suggests that the dynamics and kinetics of IFN exposure are critical parameters underlying their role in viral respiratory infections. However, the correlation between early signatures of other key anti-viral cytokines with T cell immunity has not been previously studied. Moreover, none of these combinatorial reports studied the TLR-specific functional innate immune response, which is more immune cell-specific and functional in nature than the systemic plasma levels [12].

Increased plasma IL-6, TNF-α, and IL-1β are characteristic of severe COVID-19 patients [57]. However, these cytokines have been shown to be majorly originating from infected tissues, such as the lungs, where it is possible that infiltrating innate immune cells and/or non-immune cells, such as lung endothelial cells, are their primary sources [12].

Antigen-presenting cells may also contribute to the expression of IL-1β, IL-18, and IL-23 cytokines in the plasma, as these cytokines are known to be primarily produced by antigen-presenting cells in response to the TLR/NLR signaling pathway [12,58]. Furthermore, in severe COVID-19, the peripheral innate cell expression of these proinflammatory cytokines is significantly reduced [12]. Our investigation of innate and T cell responses across the early stages of infection showed that the PBMCs from individuals with a strong proinflammatory innate immune response also exhibit a robust T cell response against SARS-CoV-2 infection. IL-18 is a proinflammatory cytokine that primarily promotes a type 1 response and activates established Th1 cells in IFN-γ production [59]. However, the correlation of proinflammatory Th17-differentiating cytokines, i.e., IL-23 and IL-1β [60], with the Th1 response in the later stages of the disease needs further investigation. Interestingly, we recently reported that IL-17A transcripts were higher at the early stage (2–4 days post-infection) of SARS-CoV-2 infection in hamsters [61]. The recent discovery of the role of the IL-23/IL-23R axis in Th1-like cells may provide the generation of potent Th1 and Th1-like cells, which may control the COVID-19 infection [62]. Therefore, it may be interesting to further investigate whether any Th1/Th17 plasticity [63] plays a role in the development of T cell response during COVID-19. Such investigations are fundamental for designing adjuvants that trigger a robust and long-lasting memory T cell immunity.

Previous studies have reported the association of late-stage proinflammatory cytokines with severe disease [64,65], and lymphocytopenia was observed in such cases [65]. However, we observed that the early induction of proinflammatory cytokines associates with a robust T cell response. Therefore, it seems likely that the impaired expression of these cytokines during the early stages of infection leads to the poor induction of antigen-specific T cells in severe cases, driving increased disease pathology. Hence, our study further underlines the critical role of the kinetics and dynamics of cytokine response in determining the clinical outcome of COVID-19. Further studies are warranted to compare these observations between mildly symptomatic and severe COVID-19 patients.

There is an orchestrated symphony between the metabolism and immune responses, where both players harmonize [66]. Although other groups have reported the longitudinal metabolomic signature [67] and single-cell transcriptomic landscape in COVID-19 patients [41,68,69], no study correlated the functional innate and T cell responses with the metabolic landscape. Our analysis found a significant correlation between the SARS-CoV-2-specific immune responses and the metabolites involved in pathways, such as arginine biosynthesis and arginine and proline metabolism. L-arginine is an immunomodulatory metabolite that plays a critical role in the pathways involving inflammation, immune regulation, and via its metabolism, leading to the generation of nitric oxide (NO), which plays an intrinsic role in Th cell activation, differentiation, survival, and proliferation [70–72]. Notably, the metabolites involved in arginine biosynthesis have been reported to be significantly altered in severe COVID-19 patients [67], and their levels are inversely correlated to the severity of COVID-19 [73]. Shen et al. reported that the metabolites involved in arginine metabolism were significantly reduced in the COVID-19 patients; in contrast, we observed that these metabolites were elevated in COVID-19-infected individuals, compared to the healthy controls (Figure S5). Such differences may be attributed to our study's predominantly asymptomatic or mildly symptomatic cohort, which further underlines the significance of metabolites involved in arginine metabolism in COVID-19 severity. Furthermore, a randomized, double-blind, placebo-controlled trial on patients hospitalized for severe COVID-19 reported that adding oral l-arginine to standard therapy in patients with severe COVID-19 significantly decreased the length of hospitalization at ten days after starting treatment [74]. These reports appear to go against the previously suggested strategy of l-arginine depletion in COVID-19, based on the premise that l-arginine is a key nutrient that is essential in the lifecycle of SARS-CoV-2 [75]. We speculate that, given the role of arginine biosynthesis metabolites in inducing a more potent T cell response, l-arginine supplementation could also be beneficial in COVID-19 vaccination and booster doses to induce long-term immunity.

The immunomodulatory effects of metabolites, such as adenosine [76], itaconate [77–79], and L-proline [80,81], have been reported independently or in the context of disease pathogenesis. Enrichment of these metabolites, as correlative markers of anti-SARS-CoV-2 immune responses, further underlines their importance in immunomodulatory mechanisms.

To conclude, our study highlights the importance of the T cell response against the emerging variants of SARS-CoV-2. We show how PBMC-derived innate responses are critical for generating a robust T cell response and how plasma metabolites correlate with the innate and adaptive immune responses. How these metabolites could act as potential immunomodulators needs further examination.

Supplementary Materials: The following supporting information can be downloaded at: https://www.mdpi.com/article/10.3390/vaccines10101762/s1, Figure S1: Gating Strategy; Figure S2: SARS-CoV-2 virus-specific innate immune responses; Figure S3: Longitudinal Analysis of IgG and IgM Response against the SARS-CoV-2 during acute COVID-19 Infection; Figure S4: Normalized Box plots and kernel density plots using the online tool Metaboanalyst 5.0; Figure S5: Normalized Box plots of representative plasma metabolites; Figure S6: SARS-CoV-2 Spike Peptide Pool Specific Cytokine Release by PBMC samples of V3; Figure S7. Longitudinal dynamics of antigen-specific cytokine release by PBMCs during COVID-19 infection; Table S1: Donor Characteristics; Table S2: List of dominant epitopes.

Author Contributions: Conceptualization, A.B., D.K.R. and A.A.; data curation, S.M., Y.K., D.K.R. and A.A.; funding acquisition, D.K.R. and A.A.; investigation, S.M., T.S., Y.K., D.K.R. and A.A.; methodology, A.B., A.Z., J.D., S.K.G., S.M., M.R.T., U.M., T.S. and Y.K.; project administration, A.K.P., D.K.R. and A.A.; supervision, A.K.P., D.K.R., and A.A.; visualization, A.B.; writing—original draft, A.B. and A.Z.; writing—review and editing, A.A. All authors have read and agreed to the published version of the manuscript.

Funding: The study was funded by BIRAC, Department of Biotechnology, through the Mission COVID Suraksha grant (BT/CS0010/CS/02/20).

Institutional Review Board Statement: All the experiments were performed according to the suggested guidelines of the Institutional Ethics Committee (human research) of THSTI and ESIC Hospital, Faridabad (letter Ref No: THS 1.8.1 (97), dated 7 July 2020). Human blood samples were collected from COVID-19 patients and healthy individuals after the written informed consent. Individuals were enrolled in this study based on the inclusion/exclusion criteria prescribed by the Institutional Ethics Committee (human research) of THSTI.

Informed Consent Statement: Informed consent was obtained from all individual participants included in the study.

Data Availability Statement: The datasets generated during and/or analyzed during the current study are available from the corresponding author, A.A., on reasonable request.

Acknowledgments: We acknowledge the funding through the Mission COVID Suraksha grant (BT/CS0010/CS/02/20) from BIRAC, Department of Biotechnology, for enabling this study. We thank all the volunteers who donated their blood samples for this study. We sincerely thank the staff and students of the Translational Health Science and Technology Institute (THSTI; Faridabad, India) for helping to ensure the smooth conduct of the study.

Conflicts of Interest: The authors declare no conflict of interest.

References

1. Stephens, D.S.; McElrath, M.J. COVID-19 and the Path to Immunity. *JAMA* **2020**, *324*, 1279–1281. [CrossRef] [PubMed]
2. Sherina, N.; Piralla, A.; Du, L.; Wan, H.; Kumagai-Braesch, M.; Andréll, J.; Braesch-Andersen, S.; Cassaniti, I.; Percivalle, E.; Sarasini, A.; et al. Persistence of SARS-CoV-2-specific B and T cell responses in convalescent COVID-19 patients 6–8 months after the infection. *Med* **2021**, *2*, 281–295.e4. [CrossRef] [PubMed]
3. Grifoni, A.; Sidney, J.; Vita, R.; Peters, B.; Crotty, S.; Weiskopf, D.; Sette, A. SARS-CoV-2 human T cell epitopes: Adaptive immune response against COVID-19. *Cell Host Microbe* **2021**, *29*, 1076–1092. [CrossRef] [PubMed]
4. Gao, Y.; Cai, C.; Grifoni, A.; Müller, T.R.; Niessl, J.; Olofsson, A.; Humbert, M.; Hansson, L.; Österborg, A.; Bergman, P.; et al. Ancestral SARS-CoV-2-specific T cells cross-recognize the Omicron variant. *Nat. Med.* **2022**, *28*, 472–476. [CrossRef]

5. Keeton, R.; Tincho, M.B.; Ngomti, A.; Baguma, R.; Benede, N.; Suzuki, A.; Khan, K.; Cele, S.; Bernstein, M.; Karim, F.; et al. T cell responses to SARS-CoV-2 spike cross-recognize Omicron. *Nature* **2022**, *603*, 488–492. [CrossRef]
6. Tarke, A.; Coelho, C.H.; Zhang, Z.; Dan, J.M.; Yu, E.D.; Methot, N.; Bloom, N.I.; Goodwin, B.; Phillips, E.; Mallal, S.; et al. SARS-CoV-2 vaccination induces immunological T cell memory able to cross-recognize variants from Alpha to Omicron. *Cell* **2022**, *185*, 847–859.e11. [CrossRef]
7. Le Bert, N.; Tan, A.T.; Kunasegaran, K.; Tham, C.Y.L.; Hafezi, M.; Chia, A.; Chng, M.H.Y.; Lin, M.; Tan, N.; Linster, M.; et al. SARS-CoV-2-specific T cell immunity in cases of COVID-19 and SARS, and uninfected controls. *Nature* **2020**, *584*, 457–462. [CrossRef]
8. Schultze, J.L.; Aschenbrenner, A.C. COVID-19 and the human innate immune system. *Cell* **2021**, *184*, 1671–1692. [CrossRef]
9. Mathew, D.; Giles, J.R.; Baxter, A.E.; Oldridge, D.A.; Greenplate, A.R.; Wu, J.E.; Alanio, C.; Kuri-Cervantes, L.; Pampena, M.B.; D'Andrea, K.; et al. Deep immune profiling of COVID-19 patients reveals distinct immunotypes with therapeutic implications. *Science* **2020**, *369*, eabc8511. [CrossRef]
10. Rydyznski Moderbacher, C.; Ramirez, S.I.; Dan, J.M.; Grifoni, A.; Hastie, K.M.; Weiskopf, D.; Belanger, S.; Abbott, R.K.; Kim, C.; Choi, J.; et al. Antigen-Specific Adaptive Immunity to SARS-CoV-2 in Acute COVID-19 and Associations with Age and Disease Severity. *Cell* **2020**, *183*, 996–1012.e9. [CrossRef]
11. Dalal, R.; Sadhu, S.; Awasthi, A. Chapter 6—Role of Th17 cell in tissue inflammation and organ-specific autoimmunity. In *Translational Autoimmunity*; Rezaei, N., Ed.; Academic Press: Cambridge, MA, USA, 2022; Volume 1, pp. 93–121.
12. Arunachalam, P.S.; Wimmers, F.; Mok, C.K.P.; Perera, R.; Scott, M.; Hagan, T.; Sigal, N.; Feng, Y.; Bristow, L.; Tak-Yin Tsang, O.; et al. Systems biological assessment of immunity to mild versus severe COVID-19 infection in humans. *Science* **2020**, *369*, 1210–1220. [CrossRef]
13. Capelle, C.M.; Ciré, S.; Domingues, O.; Ernens, I.; Hedin, F.; Fischer, A.; Snoeck, C.J.; Ammerlaan, W.; Konstantinou, M.; Grzyb, K.; et al. Combinatorial analysis reveals highly coordinated early-stage immune reactions that predict later antiviral immune responses in mild COVID-19 patients. *Cell Rep. Med.* **2022**, *4*, 100600. [CrossRef]
14. Chandran, A.; Rosenheim, J.; Nageswaran, G.; Swadling, L.; Pollara, G.; Gupta, R.K.; Burton, A.R.; Guerra-Assunção, J.A.; Woolston, A.; Ronel, T.; et al. Rapid synchronous type 1 IFN and virus-specific T cell responses characterize first wave non-severe SARS-CoV-2 infections. *Cell Rep. Med.* **2022**, *3*, 100557. [CrossRef]
15. Lee, J.W.; Su, Y.; Baloni, P.; Chen, D.; Pavlovitch-Bedzyk, A.J.; Yuan, D.; Duvvuri, V.R.; Ng, R.H.; Choi, J.; Xie, J.; et al. Integrated analysis of plasma and single immune cells uncovers metabolic changes in individuals with COVID-19. *Nat. Biotechnol.* **2022**, *40*, 110–120. [CrossRef]
16. Rendeiro, A.F.; Vorkas, C.K.; Krumsiek, J.; Singh, H.K.; Kapadia, S.N.; Cappelli, L.V.; Cacciapuoti, M.T.; Inghirami, G.; Elemento, O.; Salvatore, M. Metabolic and Immune Markers for Precise Monitoring of COVID-19 Severity and Treatment. *Front. Immunol.* **2022**, *12*, 809937. [CrossRef]
17. O'Carroll, S.M.; O'Neill, L.A.J. Targeting immunometabolism to treat COVID-19. *Immunother. Adv.* **2021**, *1*, ltab013. [CrossRef]
18. Khwatenge, C.N.; Pate, M.; Miller, L.C.; Sang, Y. Immunometabolic Dysregulation at the Intersection of Obesity and COVID-19. *Front. Immunol.* **2021**, *12*, 732913. [CrossRef] [PubMed]
19. Siska, P.J.; Decking, S.-M.; Babl, N.; Matos, C.; Bruss, C.; Singer, K.; Klitzke, J.; Schön, M.; Simeth, J.; Köstler, J.; et al. Metabolic imbalance of T cells in COVID-19 is hallmarked by basigin and mitigated by dexamethasone. *J. Clin. Investig.* **2021**, *131*, e148225. [CrossRef] [PubMed]
20. Chaudhuri, S.; Thiruvengadam, R.; Chattopadhyay, S.; Mehdi, F.; Kshetrapal, P.; Shrivastava, T.; Desiraju, B.K.; Batra, G.; Kang, G.; Bhatnagar, S. Comparative evaluation of SARS-CoV-2 IgG assays in India. *J. Clin. Virol.* **2020**, *131*, 104609. [CrossRef] [PubMed]
21. Thiruvengadam, R.; Awasthi, A.; Medigeshi, G.; Bhattacharya, S.; Mani, S.; Sivasubbu, S.; Shrivastava, T.; Samal, S.; Rathna Murugesan, D.; Koundinya Desiraju, B.; et al. Effectiveness of ChAdOx1 nCoV-19 vaccine against SARS-CoV-2 infection during the delta (B.1.617.2) variant surge in India: A test-negative, case-control study and a mechanistic study of post-vaccination immune responses. *Lancet Infect. Dis.* **2021**, *22*, 473–482. [CrossRef]
22. Dan, J.M.; Mateus, J.; Kato, Y.; Hastie, K.M.; Yu, E.D.; Faliti, C.E.; Grifoni, A.; Ramirez, S.I.; Haupt, S.; Frazier, A.; et al. Immunological memory to SARS-CoV-2 assessed for up to 8 months after infection. *Science* **2021**, *371*, eabf4063. [CrossRef] [PubMed]
23. Naz, S.; Gallart-Ayala, H.; Reinke, S.N.; Mathon, C.; Blankley, R.; Chaleckis, R.; Wheelock, C.E. Development of a Liquid Chromatography–High Resolution Mass Spectrometry Metabolomics Method with High Specificity for Metabolite Identification Using All Ion Fragmentation Acquisition. *Anal. Chem.* **2017**, *89*, 7933–7942. [CrossRef] [PubMed]
24. Kumar, A.; Kumar, Y.; Sevak, J.K.; Kumar, S.; Kumar, N.; Gopinath, S.D. Metabolomic analysis of primary human skeletal muscle cells during myogenic progression. *Sci. Rep.* **2020**, *10*, 11824. [CrossRef]
25. Sadhu, S.; Rizvi, Z.A.; Pandey, R.P.; Dalal, R.; Rathore, D.K.; Kumar, B.; Pandey, M.; Kumar, Y.; Goel, R.; Maiti, T.K.; et al. Gefitinib Results in Robust Host-Directed Immunity Against Salmonella Infection Through Proteo-Metabolomic Reprogramming. *Front. Immunol.* **2021**, *12*, 648710. [CrossRef]
26. Rizvi, Z.A.; Dalal, R.; Sadhu, S.; Kumar, Y.; Kumar, S.; Gupta, S.K.; Tripathy, M.R.; Rathore, D.K.; Awasthi, A. High-salt diet mediates interplay between NK cells and gut microbiota to induce potent tumor immunity. *Sci. Adv.* **2021**, *7*, eabg5016. [CrossRef] [PubMed]

27. Goedhart, J.; Luijsterburg, M.S. VolcaNoseR is a web app for creating, exploring, labeling and sharing volcano plots. *Sci. Rep.* **2020**, *10*, 20560. [CrossRef]
28. Chong, J.; Soufan, O.; Li, C.; Caraus, I.; Li, S.; Bourque, G.; Wishart, D.S.; Xia, J. MetaboAnalyst 4.0: Towards more transparent and integrative metabolomics analysis. *Nucleic Acids Res.* **2018**, *46*, W486–W494. [CrossRef]
29. Isho, B.; Abe, K.T.; Zuo, M.; Jamal, A.J.; Rathod, B.; Wang, J.H.; Li, Z.; Chao, G.; Rojas, O.L.; Bang, Y.M.; et al. Persistence of serum and saliva antibody responses to SARS-CoV-2 spike antigens in COVID-19 patients. *Sci. Immunol.* **2020**, *5*, eabb551. [CrossRef]
30. Planas, D.; Veyer, D.; Baidaliuk, A.; Staropoli, I.; Guivel-Benhassine, F.; Rajah, M.M.; Planchais, C.; Porrot, F.; Robillard, N.; Puech, J.; et al. Reduced sensitivity of SARS-CoV-2 variant Delta to antibody neutralization. *Nature* **2021**, *596*, 276–280. [CrossRef]
31. Sahin, U.; Muik, A.; Derhovanessian, E.; Vogler, I.; Kranz, L.M.; Vormehr, M.; Baum, A.; Pascal, K.; Quandt, J.; Maurus, D.; et al. COVID-19 vaccine BNT162b1 elicits human antibody and TH1 T cell responses. *Nature* **2020**, *586*, 594–599. [CrossRef]
32. Grifoni, A.; Weiskopf, D.; Ramirez, S.I.; Mateus, J.; Dan, J.M.; Moderbacher, C.R.; Rawlings, S.A.; Sutherland, A.; Premkumar, L.; Jadi, R.S.; et al. Targets of T Cell Responses to SARS-CoV-2 Coronavirus in Humans with COVID-19 Disease and Unexposed Individuals. *Cell* **2020**, *181*, 1489–1501.e15. [CrossRef] [PubMed]
33. Diamond, M.S.; Kanneganti, T.-D. Innate immunity: The first line of defense against SARS-CoV-2. *Nat. Immunol.* **2022**, *23*, 165–176. [CrossRef] [PubMed]
34. Krieg, A.M.; Vollmer, J. Toll-like receptors 7, 8, and 9: Linking innate immunity to autoimmunity. *Immunol. Rev.* **2007**, *220*, 251–269. [CrossRef]
35. Danlos, F.-X.; Grajeda-Iglesias, C.; Durand, S.; Sauvat, A.; Roumier, M.; Cantin, D.; Colomba, E.; Rohmer, J.; Pommeret, F.; Baciarello, G.; et al. Metabolomic analyses of COVID-19 patients unravel stage-dependent and prognostic biomarkers. *Cell Death Dis.* **2021**, *12*, 258. [CrossRef]
36. Jia, H.; Liu, C.; Li, D.; Huang, Q.; Liu, D.; Zhang, Y.; Ye, C.; Zhou, D.; Wang, Y.; Tan, Y.; et al. Metabolomic analyses reveals new stage-specific features of the COVID-19. *Eur. Respir. J.* **2021**, *59*, 2100284. [CrossRef]
37. Páez-Franco, J.C.; Torres-Ruiz, J.; Sosa-Hernández, V.A.; Cervantes-Díaz, R.; Romero-Ramírez, S.; Pérez-Fragoso, A.; Meza-Sánchez, D.E.; Germán-Acacio, J.M.; Maravillas-Montero, J.L.; Mejía-Domínguez, N.R.; et al. Metabolomics analysis reveals a modified amino acid metabolism that correlates with altered oxygen homeostasis in COVID-19 patients. *Sci. Rep.* **2021**, *11*, 6350. [CrossRef]
38. Sindelar, M.; Stancliffe, E.; Schwaiger-Haber, M.; Anbukumar, D.S.; Adkins-Travis, K.; Goss, C.W.; O'Halloran, J.A.; Mudd, P.A.; Liu, W.-C.; Albrecht, R.A.; et al. Longitudinal metabolomics of human plasma reveals prognostic markers of COVID-19 disease severity. *Cell Rep. Med.* **2021**, *2*, 100369. [CrossRef]
39. Flor, L.S.; Friedman, J.; Spencer, C.N.; Cagney, J.; Arrieta, A.; Herbert, M.E.; Stein, C.; Mullany, E.C.; Hon, J.; Patwardhan, V.; et al. Quantifying the effects of the COVID-19 pandemic on gender equality on health, social, and economic indicators: A comprehensive review of data from March, 2020, to September, 2021. *Lancet* **2022**, *399*, 2381–2397. [CrossRef]
40. Wilk, A.J.; Lee, M.J.; Wei, B.; Parks, B.; Pi, R.; Martínez-Colón, G.J.; Ranganath, T.; Zhao, N.Q.; Taylor, S.; Becker, W.; et al. Multi-omic profiling reveals widespread dysregulation of innate immunity and hematopoiesis in COVID-19. *J. Exp. Med.* **2021**, *218*, e20210582. [CrossRef]
41. Stephenson, E.; Reynolds, G.; Botting, R.A.; Calero-Nieto, F.J.; Morgan, M.D.; Tuong, Z.K.; Bach, K.; Sungnak, W.; Worlock, K.B.; Yoshida, M.; et al. Single-cell multi-omics analysis of the immune response in COVID-19. *Nat. Med.* **2021**, *27*, 904–916. [CrossRef] [PubMed]
42. Barh, D.; Tiwari, S.; Andrade, B.S.; Weener, M.E.; Góes-Neto, A.; Azevedo, V.; Ghosh, P.; Blum, K.; Ganguly, N.K. A novel multi-omics-based highly accurate prediction of symptoms, comorbid conditions, and possible long-term complications of COVID-19. *Mol. Omics* **2021**, *17*, 317–337. [CrossRef] [PubMed]
43. Tan, A.T.; Linster, M.; Tan, C.W.; Le Bert, N.; Chia, W.N.; Kunasegaran, K.; Zhuang, Y.; Tham, C.Y.L.; Chia, A.; Smith, G.J.D.; et al. Early induction of functional SARS-CoV-2-specific T cells associates with rapid viral clearance and mild disease in COVID-19 patients. *Cell Rep.* **2021**, *34*, 108728. [CrossRef]
44. Hadjadj, J.; Yatim, N.; Barnabei, L.; Corneau, A.; Boussier, J.; Smith, N.; Péré, H.; Charbit, B.; Bondet, V.; Chenevier-Gobeaux, C.; et al. Impaired type I interferon activity and inflammatory responses in severe COVID-19 patients. *Science* **2020**, *369*, 718–724. [CrossRef]
45. Wang, Z.; Pan, H.; Jiang, B. Type I IFN deficiency: An immunological characteristic of severe COVID-19 patients. *Signal Transduct. Target. Ther.* **2020**, *5*, 198. [CrossRef]
46. Thiruvengadam, R.; Binayke, A.; Awasthi, A. SARS-CoV-2 delta variant: A persistent threat to the effectiveness of vaccines. *Lancet Infect. Dis.* **2022**, *22*. [CrossRef]
47. Nyberg, T.; Ferguson, N.M.; Nash, S.G.; Webster, H.H.; Flaxman, S.; Andrews, N.; Hinsley, W.; Bernal, J.L.; Kall, M.; Bhatt, S.; et al. Comparative analysis of the risks of hospitalisation and death associated with SARS-CoV-2 omicron (B.1.1.529) and delta (B.1.617.2) variants in England: A cohort study. *Lancet* **2022**, *399*, 1303–1312. [CrossRef]
48. Liu, J.; Chandrashekar, A.; Sellers, D.; Barrett, J.; Jacob-Dolan, C.; Lifton, M.; McMahan, K.; Sciacca, M.; VanWyk, H.; Wu, C.; et al. Vaccines elicit highly conserved cellular immunity to SARS-CoV-2 Omicron. *Nature* **2022**, *603*, 493–496. [CrossRef] [PubMed]
49. Tennøe, S.; Gheorghe, M.; Stratford, R.; Clancy, T. The T cell epitope landscape of SARS-CoV-2 variants of concern. *Vaccines* **2022**, *10*, 1123. [CrossRef]

50. Harvey, W.T.; Carabelli, A.M.; Jackson, B.; Gupta, R.K.; Thomson, E.C.; Harrison, E.M.; Ludden, C.; Reeve, R.; Rambaut, A.; Peacock, S.J.; et al. SARS-CoV-2 variants, spike mutations and immune escape. *Nat. Rev. Microbiol.* **2021**, *19*, 409–424. [CrossRef] [PubMed]
51. Shah, M.; Woo, H.G. Omicron: A Heavily Mutated SARS-CoV-2 Variant Exhibits Stronger Binding to ACE2 and Potently Escapes Approved COVID-19 Therapeutic Antibodies. *Front. Immunol.* **2022**, *12*, 830527. [CrossRef] [PubMed]
52. Gil-Etayo, F.J.; Garcinuño, S.; Utrero-Rico, A.; Cabrera-Marante, O.; Arroyo-Sanchez, D.; Mancebo, E.; Pleguezuelo, D.E.; Rodríguez-Frías, E.; Allende, L.M.; Morales-Pérez, P. An Early Th1 Response Is a Key Factor for a Favorable COVID-19 Evolution. *Biomedicines* **2022**, *10*, 296. [CrossRef] [PubMed]
53. Janssen, N.A.F.; Grondman, I.; de Nooijer, A.H.; Boahen, C.K.; Koeken, V.; Matzaraki, V.; Kumar, V.; He, X.; Kox, M.; Koenen, H.; et al. Dysregulated Innate and Adaptive Immune Responses Discriminate Disease Severity in COVID-19. *J. Infect. Dis.* **2021**, *223*, 1322–1333. [CrossRef] [PubMed]
54. Masood, K.I.; Yameen, M.; Ashraf, J.; Shahid, S.; Mahmood, S.F.; Nasir, A.; Nasir, N.; Jamil, B.; Ghanchi, N.K.; Khanum, I.; et al. Upregulated type I interferon responses in asymptomatic COVID-19 infection are associated with improved clinical outcome. *Sci. Rep.* **2021**, *11*, 22958. [CrossRef] [PubMed]
55. Bastard, P.; Rosen, L.B.; Zhang, Q.; Michailidis, E.; Hoffmann, H.-H.; Zhang, Y.; Dorgham, K.; Philippot, Q.; Rosain, J.; Béziat, V.; et al. Autoantibodies against type I IFNs in patients with life-threatening COVID-19. *Science* **2020**, *370*, eabd4585. [CrossRef] [PubMed]
56. Alavi Darazam, I.; Shokouhi, S.; Pourhoseingholi, M.A.; Naghibi Irvani, S.S.; Mokhtari, M.; Shabani, M.; Amirdosara, M.; Torabinavid, P.; Golmohammadi, M.; Hashemi, S.; et al. Role of interferon therapy in severe COVID-19: The COVIFERON randomized controlled trial. *Sci. Rep.* **2021**, *11*, 8059. [CrossRef]
57. Del Valle, D.M.; Kim-Schulze, S.; Huang, H.-H.; Beckmann, N.D.; Nirenberg, S.; Wang, B.; Lavin, Y.; Swartz, T.H.; Madduri, D.; Stock, A.; et al. An inflammatory cytokine signature predicts COVID-19 severity and survival. *Nat. Med.* **2020**, *26*, 1636–1643. [CrossRef]
58. Liu, T.; Zhang, L.; Joo, D.; Sun, S.-C. NF-κB signaling in inflammation. *Signal Transduct. Target. Ther.* **2017**, *2*, 17023. [CrossRef]
59. Nakanishi, K. Unique action of interleukin-18 on T cells and other immune cells. *Front. Immunol.* **2018**, *9*, 763. [CrossRef]
60. Lee, Y.; Awasthi, A.; Yosef, N.; Quintana, F.J.; Xiao, S.; Peters, A.; Wu, C.; Kleinewietfeld, M.; Kunder, S.; Hafler, D.A.; et al. Induction and molecular signature of pathogenic TH17 cells. *Nat. Immunol.* **2012**, *13*, 991–999. [CrossRef]
61. Rizvi, Z.A.; Dalal, R.; Sadhu, S.; Binayke, A.; Dandotiya, J.; Kumar, Y.; Shrivastava, T.; Gupta, S.K.; Aggarwal, S.; Tripathy, M.R.; et al. Golden Syrian hamster as a model to study cardiovascular complications associated with SARS-CoV-2 infection. *eLife* **2022**, *11*, e73522. [CrossRef]
62. Pawlak, M.; DeTomaso, D.; Schnell, A.; Meyer zu Horste, G.; Lee, Y.; Nyman, J.; Dionne, D.; Regan, B.M.L.; Singh, V.; Delorey, T.; et al. Induction of a colitogenic phenotype in Th1-like cells depends on interleukin-23 receptor signaling. *Immunity* **2022**, *55*, 1663–1679. [CrossRef]
63. DuPage, M.; Bluestone, J.A. Harnessing the plasticity of CD4+ T cells to treat immune-mediated disease. *Nat. Rev. Immunol.* **2016**, *16*, 149–163. [CrossRef]
64. Lau, S.K.; Lau, C.C.; Chan, K.-H.; Li, C.P.; Chen, H.; Jin, D.-Y.; Chan, J.F.; Woo, P.C.; Yuen, K.-Y. Delayed induction of proinflammatory cytokines and suppression of innate antiviral response by the novel Middle East respiratory syndrome coronavirus: Implications for pathogenesis and treatment. *J. Gen. Virol.* **2013**, *94*, 2679–2690. [CrossRef]
65. Ye, Q.; Wang, B.; Mao, J. The pathogenesis and treatment of the 'Cytokine Storm' in COVID-19. *J. Infect.* **2020**, *80*, 607–613. [CrossRef]
66. Wculek, S.K.; Khouili, S.C.; Priego, E.; Heras-Murillo, I.; Sancho, D. Metabolic Control of Dendritic Cell Functions: Digesting Information. *Front. Immunol.* **2019**, *10*, 775. [CrossRef] [PubMed]
67. Ansone, L.; Briviba, M.; Silamikelis, I.; Terentjeva, A.; Perkons, I.; Birzniece, L.; Rovite, V.; Rozentale, B.; Viksna, L.; Kolesova, O.; et al. Amino Acid Metabolism is Significantly Altered at the Time of Admission in Hospital for Severe COVID-19 Patients: Findings from Longitudinal Targeted Metabolomics Analysis. *Microbiol. Spectr.* **2021**, *9*, e00338-00321. [CrossRef] [PubMed]
68. Fischer, D.S.; Ansari, M.; Wagner, K.I.; Jarosch, S.; Huang, Y.; Mayr, C.H.; Strunz, M.; Lang, N.J.; D'Ippolito, E.; Hammel, M.; et al. Single-cell RNA sequencing reveals ex vivo signatures of SARS-CoV-2-reactive T cells through 'reverse phenotyping'. *Nat. Commun.* **2021**, *12*, 4515. [CrossRef]
69. Meckiff, B.J.; Ramírez-Suástegui, C.; Fajardo, V.; Chee, S.J.; Kusnadi, A.; Simon, H.; Eschweiler, S.; Grifoni, A.; Pelosi, E.; Weiskopf, D.; et al. Imbalance of Regulatory and Cytotoxic SARS-CoV-2-Reactive CD4(+) T Cells in COVID-19. *Cell* **2020**, *183*, 1340–1353. [CrossRef]
70. Bronte, V.; Zanovello, P. Regulation of immune responses by L-arginine metabolism. *Nat. Rev. Immunol.* **2005**, *5*, 641–654. [CrossRef]
71. Kishton Rigel, J.; Sukumar, M.; Restifo Nicholas, P. Arginine Arms T Cells to Thrive and Survive. *Cell Metab.* **2016**, *24*, 647–648. [CrossRef] [PubMed]
72. Kim, S.-H.; Roszik, J.; Grimm, E.A.; Ekmekcioglu, S. Impact of l-arginine metabolism on immune response and anticancer immunotherapy. *Front. Oncol.* **2018**, *8*, 67. [CrossRef]

73. Sacchi, A.; Grassi, G.; Notari, S.; Gili, S.; Bordoni, V.; Tartaglia, E.; Casetti, R.; Cimini, E.; Mariotti, D.; Garotto, G. Expansion of myeloid derived suppressor cells contributes to platelet activation by L-arginine deprivation during SARS-CoV-2 infection. *Cells* **2021**, *10*, 2111. [CrossRef] [PubMed]
74. Fiorentino, G.; Coppola, A.; Izzo, R.; Annunziata, A.; Bernardo, M.; Lombardi, A.; Trimarco, V.; Santulli, G.; Trimarco, B. Effects of adding L-arginine orally to standard therapy in patients with COVID-19: A randomized, double-blind, placebo-controlled, parallel-group trial. Results of the first interim analysis. *eClinicalMedicine* **2021**, *40*, 101125. [CrossRef] [PubMed]
75. Grimes, J.M.; Khan, S.; Badeaux, M.; Rao, R.M.; Rowlinson, S.W.; Carvajal, R.D. Arginine depletion as a therapeutic approach for patients with COVID-19. *Int. J. Infect. Dis.* **2021**, *102*, 566–570. [CrossRef]
76. Buck, M.D.; O'Sullivan, D.; Pearce, E.L. T cell metabolism drives immunity. *J. Exp. Med.* **2015**, *212*, 1345–1360. [CrossRef]
77. Swain, A.; Bambouskova, M.; Kim, H.; Andhey, P.S.; Duncan, D.; Auclair, K.; Chubukov, V.; Simons, D.M.; Roddy, T.P.; Stewart, K.M.; et al. Comparative evaluation of itaconate and its derivatives reveals divergent inflammasome and type I interferon regulation in macrophages. *Nat. Metab.* **2020**, *2*, 594–602. [CrossRef]
78. Mills, E.L.; Ryan, D.G.; Prag, H.A.; Dikovskaya, D.; Menon, D.; Zaslona, Z.; Jedrychowski, M.P.; Costa, A.S.H.; Higgins, M.; Hams, E.; et al. Itaconate is an anti-inflammatory metabolite that activates Nrf2 via alkylation of KEAP1. *Nature* **2018**, *556*, 113–117. [CrossRef] [PubMed]
79. Kobayashi, E.H.; Suzuki, T.; Funayama, R.; Nagashima, T.; Hayashi, M.; Sekine, H.; Tanaka, N.; Moriguchi, T.; Motohashi, H.; Nakayama, K.; et al. Nrf2 suppresses macrophage inflammatory response by blocking proinflammatory cytokine transcription. *Nat. Commun.* **2016**, *7*, 11624. [CrossRef]
80. Ye, L.; Park, J.J.; Peng, L.; Yang, Q.; Chow, R.D.; Dong, M.B.; Lam, S.Z.; Guo, J.; Tang, E.; Zhang, Y.; et al. A genome-scale gain-of-function CRISPR screen in CD8 T cells identifies proline metabolism as a means to enhance CAR-T therapy. *Cell Metab* **2022**, *34*, 595–614.e514. [CrossRef]
81. Vita, R.; Mahajan, S.; Overton, J.A.; Dhanda, S.K.; Martini, S.; Cantrell, J.R.; Wheeler, D.K.; Sette, A.; Peters, B. The immune epitope database (IEDB): 2018 update. *Nucleic Acids Res.* **2019**, *47*, D339–D343. [CrossRef]